Ab initio calculations of zirconium adsorption and diffusion on graphene

Y. Sanchez-Paisal, D. Sanchez-Portal, and A. Ayuela
Departamento de Física de Materiales, Facultad de Químicas, Centro de Física de Materiales CFM-MPC, and Donostia International Physics Center (DIPC), Universidad del País Vasco, P.O. Box 1072, 20018 San Sebastian/Donostia, Spain
(Received 29 May 2009; revised manuscript received 8 July 2009; published 30 July 2009)

We report *ab initio* calculations of zirconium-coated graphene sheets at several coverages and geometries. We calculate adsorption properties, such as distances and the Zr/graphene binding energies. When increasing the Zr/C coverage ratio, the binding energies show that the Zr atoms have a trend to cluster. The most stable Zr/C coverage corresponds to 0.375, which has no stress between the zirconium and graphene layer. The Zr-graphene binding involves charge transfer to graphene which comes from the 5*s* orbital of Zr and depends on the coverage. We also calculate the diffusion-energy barriers on graphene for the single atom and the Zr_3 trimer and we see that the Zr_3 cluster is a faster diffusion unit. We also estimate that the Zr diffusion energy between two substitutional positions is at least 4 eV, which is large enough to fix Zr atoms bound to C vacancies at actual temperatures in high-resolution transmission electronic microscopy experiments.

DOI: 10.1103/PhysRevB.80.045428 PACS number(s): 68.35.−p, 68.65.−k, 62.23.Kn, 68.37.Og

I. INTRODUCTION

Currently the adsorption and diffusion of different elements on carbon nanotubes[1] or graphene[2] sheets is interesting due to their great potential application[3] in nanotechnology. The mechanical properties of single-walled carbon nanotubes, with Young modulus up to 1 TPa,[4] open a new range of technological applications as reinforcing elements in nanocomposites.[5] Although many attempts have been made to develop new reinforced composite materials, the gain in many mechanical properties is not yet fully satisfactory.[6] For instance, several groups[7,8] are interested in zirconium oxide ZrO_2/carbon nanotube composites. Experiments[9–11] involving zirconium as catalyst and nanotube growth (with radii of several hundredth Å) have revealed nanocrystalline structures with zirconia grains of about 15 Å in size in the outer wall of carbon nanotubes. These nanograins originate from the formation of a ZrC layer, and could be originally related to the clustering trend of Zr atoms on large radius nanotubes.[12] Thus, further theoretical work of Zr on graphene is needed to understand this initial stage previous to the nanograin formation.

Preliminary experimental results show that Zr metal cover the multiwall nanotubes[12] when growing hydrothermally ZrO_2 with multiwall nanotubes. In that previous work we studied theoretically the Zr adsorption on graphene and its dependence with uniform coverage. The optimum theoretical Zr/C coverage was in agreement with the experimental results for multiwalled nanotubes obtained with high-resolution transmission electronic microscopy (HRTEM) and cspectroscopy. No information on the clustering of atoms for low coverages during Zr adsorption was presented.

The understanding of Zr diffusion over a graphene layer, carbon nanotubes, or graphite, is also needed to explain the ZrC-layer growth. Along this line, recent HRTEM experiments at several temperatures found also Au and Pt metals in graphenic structures, such as graphene and multiwalled nanotubes.[13] The metal atoms are substitutionally distributed in single atoms or small clusters of a few atoms (the exact number is difficult to determine). By tracking the location of metals atoms, the activation energies were obtained. Similar investigations for the diffusion of Zr atoms on and in graphene can be possible.

In this work we mainly focus on the study of ideal graphene sheets with no defects or vacancies. The role of coverage and geometrical positions is important during the adsorption. The Zr adsorption on graphene could take place at three different positions, hollow, top, and bridge, as shown in Fig. 1. A comparison between different geometries with the same coverages is done in Sec. III. The differences between a clustered or homogeneous zirconium distribution are important. The clustered coverages are found more stable for the studied cases. A discussion of the binding energies with different Zr/C coverage ratios from 0.056 to 0.5 is given in Sec. IV. A preferred coverage for Zr growth on graphene is deduced. In Sec. V, we explain in more detail from the electronic point of view the large variations in cohesive energy and Zr-C distances with coverage. The binding energies found for Zr_3 cluster motivates the study of the diffusion energy barriers for both the single Zr atom and the Zr_3 cluster, discussed in Sec. VI. Additionally, we comment on the role of graphene defects as pinning locations for the Zr adatoms. Summary and conclusions are included in Sec. VII. These simulations could be useful as a first approximation for the Zr adsorption on large radius single wall nanotubes, as in the outer layer of multiwall carbon nanotubes, and (0001) graphite surface.

II. COMPUTATIONAL DETAILS

Calculations were performed using density functional theory with the SIESTA package.[14] generalized gradient approximation for the exchange and correlation follows the Perdew-Burke-Ernzerhof form.[15] Basis sets include semicore electrons $(4s)^2(4p)^6$ for Zr and polarization orbitals for both Zr and C atoms. DZ basis set are used for each angular symmetry while the polarization orbitals are 5*p* and 3*d* for Zr and C, respectively. All the calculations were allowed to have spin polarization. The mesh cutoff and the number of *k* points were converged until the changes in energy are below

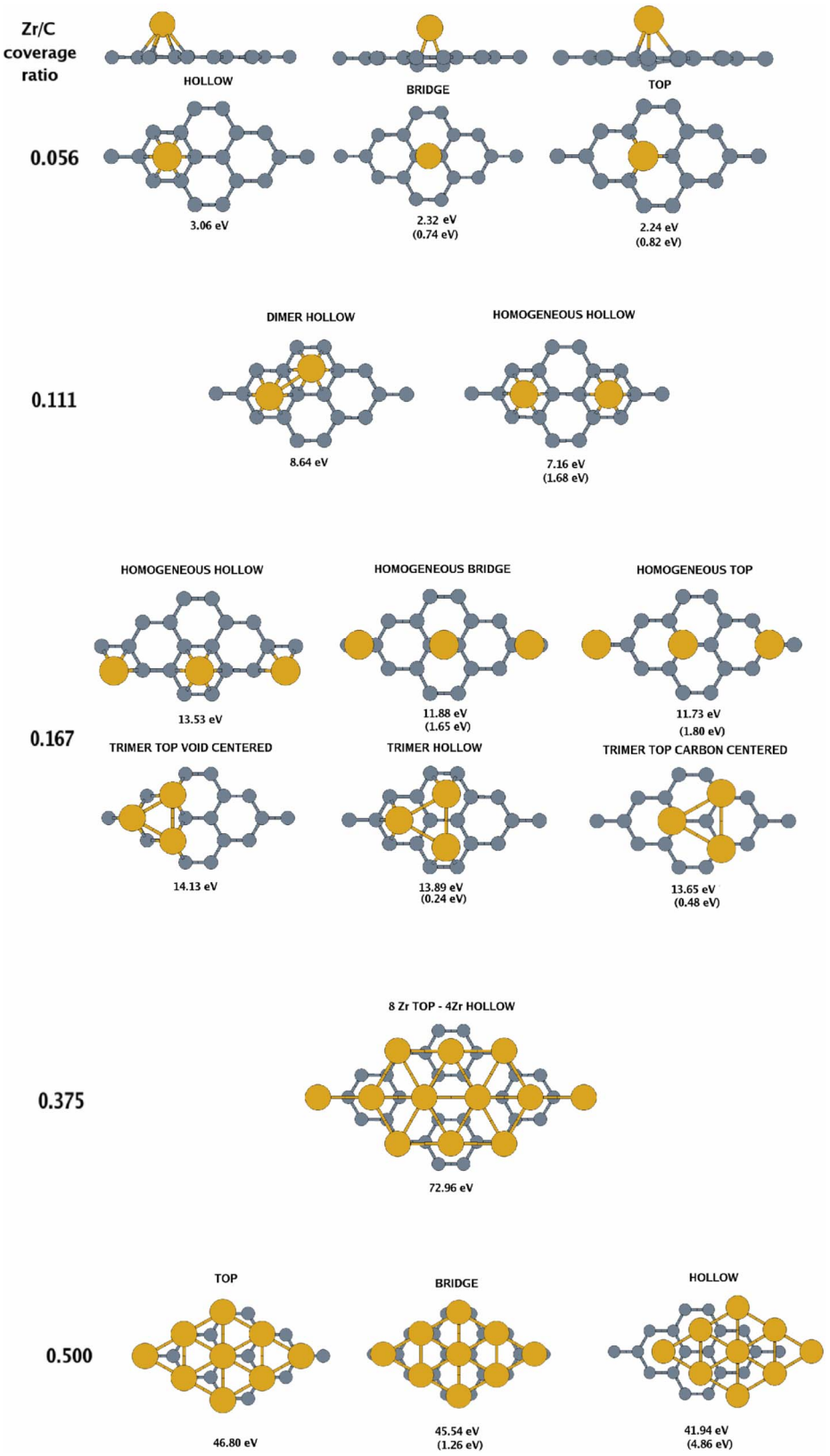

FIG. 1. (Color online) Relaxed geometries at different Zr/C coverage ratios. The total binding energies between all Zr atoms and graphene are given under each configuration. In parenthesis the energy difference respect the ground state at the studied coverages is given in eV. The clustering of Zr atoms always becomes favorable. Note the change from hollow to top positions when increasing Zr/C coverage.

0.01 eV per unit cell. We used 40 k points in the irreducible Brillouin Zone (IBZ). A mesh cutoff of 180 Ry sets the wavelength of the shortest plane wave that can be represented on the grid. Our calculations were done using 3×3 and 4×4 graphene supercells containing 18 and 32 carbon atoms at different zirconium coverages. We observe that when looking to the energy differences for some geometries, they are nearly independent of the cell used, using the previous energy-convergence criteria. Thus, in the following we present the results for the 3×3 smaller cell. The relaxed

TABLE I. Fully relaxed cell vectors of 3×3 graphene supercell at different homogeneous coverages. Their Cartesian values are given in Å.

	Cell parameters (a and b) Å		
Zr/C coverage	Hollow	Bridge	Top
0.055	$(6.477, \pm 3.740)$	$(6.452, \pm 3.717)$	$(6.462, \pm 3.731)$
0.166	$(6.432, \pm 3.713)$	$(6.375, \pm 3.710)$	$(6.398, \pm 3.694)$
0.500	$(6.834, \pm 3.945)$	$(6.827, \pm 4.009)$	$(6.912, \pm 3.990)$

geometries are shown in Fig. 1. The calculations have Zr/C coverage ratios on graphene that range between 0.056 and 0.50. The Zr atoms are arranged in clustered and homogeneous geometries at hollow, bridge, and top positions. The notation concerning these geometries is described in Fig. 1.

III. A CLOSER LOOK TO GEOMETRY: LARGE VARIATION IN ZR-C DISTANCES AND DEFORMATION OF GRAPHENE LAYER

First, we consider the geometrical parameters. We focus on (a) the cell vector variations, (b) the Zr-Zr distances for the different geometries and coverages, (c) the Zr height over the graphene, and (d) the deformations of carbon layer due to Zr adsorption. As all of our simulations have fully relaxed atomic coordinates, we can obtain valuable information about the changes in the cell vectors, the deformations of the graphene layer in every direction and the atom-atom distances. We shall comment these results in connection with strain-stress considerations, which is a way to start dealing with the system stability, to be commented at length in the next section looking to their binding energies.

A. Graphene cell-vector variations with homogeneous Zr coverage

Here, we comment on the cell vectors and the related C-C average distances. In Table I we gather the variation in the cell vectors and therefore the C-C distances. The largest deformation is at Zr/C coverage ratio of 0.5, where the C-C distances increase by about 6%. The Zr adsorption on graphene can either expand or contract these distances.

We compare these C-C graphene distances with the Zr-Zr distances in a hexagonal plane and understand how the changes in the cell vectors are related to these differences. The graphene C-C relaxed distance is 1.43 Å and the cell vectors are given by $(6.435, \pm 3.715)$ Å to be compared with values in Table I. The relaxed Zr-Zr distance on a free hexagonal (0001) plane is 2.86 Å. If the Zr-Zr distance in the simulation is larger than the 2.86 Å value, then the cell vectors are contracted. This contraction is due to the trend of the Zr atoms to reach their natural distance without graphene. The cell vector decrease occurs only at the homogeneous Zr/C coverage ratio of 0.166. If the Zr-Zr distance in the simulations is smaller, then the cell vectors are expanded. The Zr-Zr bonds are strong and the Zr-Zr distance tries to accommodate to its natural value at any coverage by expanding or contracting the underlying graphene cell. This result can be explained because the Zr-Zr bonds, after a certain cutoff distance, are stronger than the Zr-C bonds.

With these values in mind we simulated the cell where the Zr-Zr distance is nearly commensurate with the graphene plane. This configuration is the 4×4 supercell with 32 C atoms and 12 Zr atoms at a homogeneous Zr/C coverage ratio of 0.375, which corresponds to a ratio 8/4 between top and hollow states. The energetics of this configuration will be discussed later in Sec. VI. A picture of the geometry is given close to the bottom of Fig. 1.

B. Zr-Zr distances in clusters

In hollow configurations, the Zr-Zr bond distances for the dimer and the trimer become 2.60 Å and 3.08 Å, respectively. However, the top configurations of trimers have two possible geometries, as shown in Fig. 1. When the trimer lay on the graphene without a C atom in the middle, the Zr-Zr distance is 2.75 Å, and when the trimer sits on the graphene in a position where a C atom is in the center, the Zr-Zr distance is 2.94 Å. They are called top-void and top-carbon centered trimers, respectively. Snapshots of these geometries are plotted in Fig. 1.

We compare these differences between Zr-Zr distances on graphene with those for the free Zr-dimer and Zr-trimer distances. The Zr-Zr distances of free zirconium dimer and trimer are 2.09 Å and 2.60 Å, respectively. The Zr-Zr distances are always larger for the clusters supported on graphene than those for the free ones. The Zr trimer on graphene in the void centered geometry has the closer distance to the free Zr trimer, 2.60 Å versus 2.75 Å. The stress between the Zr trimer and the graphene is smaller in this case, and this geometry at a 0.166 Zr/C coverage ratio is the most stable for trimers, as seen in Fig. 1 and Sec. IV.

C. Zr height on graphene

The Zr height to the nearest C neighbors is given in Table II. The range for the Zr height is between 1.73 Å and 2.61 Å. We found large differences in the Zr height on graphene between different Zr/C coverages and geometries. We also calculated the ZrC molecule in order to compare the bond length. The Zr-C molecular distance is 1.73 Å. For every geometry and coverage the Zr height is larger than the distance for the molecule. As the coverage increases, the role of the Zr-C bond decreases and the Zr-Zr bond dominates. The Zr-C height increases with coverage for this reason. This stretching is due to the different kind of interactions between the Zr and the graphene related to the different electronic configuration, discussed later in Sec. V.

D. Deformation of graphene due to Zr adsorption

In the first three images of Fig. 1, we see how the Zr adsorption causes also height variations of the near C atoms. The deformation generated in graphene by the Zr adsorption becomes remarkable in some cases because the layer remains no longer flat. At Zr/C coverage ratio of 0.056, the highest carbon-height differences respect to graphene are 0.05 Å for

TABLE II. Average zirconium height over the plain of first-nearest C neighbors in graphene. At a clustered Zr/C coverage ratio of 0.166, it is given for the homogeneous *h* and clustered *c* geometries when applicable: on top positions, we have two different configurations (Fig. 1), as explained in the text. The Zr-C distance to graphene extends with the Zr/C coverage.

	d_{avg} (Å)		
Zr/C Coverage	Hollow [h and c]	Bridge [h and c]	Top [h and c]
0.055	1.89	1.73	2.24
0.166	1.99[h], 2.16[c]	2.14[h]	2.25[h], 2.27[c, a]/2.26[c, b]
0.500	2.61	2.46	2.38

[a]Trimer void centered.
[b]Trimer top-carbon centered.

the hollow position, 0.15 Å for the bridge configuration and 0.32 Å for the top adsorption. The deformation sinks the C atoms under the Zr. This effect is in agreement with the wrapping of carbon atoms around other early transition element with 5*d* electrons.[16] This sinking deformation is reversed for carbon adatoms on graphene.[17] This difference can be explained because the in principle C-Zr covalent bond has some extra peculiarities, such as its partial ionicity, at which we shall look in Sec. V with more detail.

IV. BINDING ENERGIES: CLUSTERING EFFECT OF ZR ATOMS ON GRAPHENE

Next, we analyze the binding energies of Zr attached to the graphene layer as a function of coverage. The binding energy E_B for Zr coating graphene is given as

$$E_{B_{\text{Zr-Graphene}}} = -(E_{\text{Zr-graphene}} - E_{\text{graphene}} - n_{\text{Zr}}E_{\text{Zr}}), \qquad (1)$$

where $E_{\text{Zr-graphene}}$ is the total energy of graphene with Zr coverage, E_{graphene} is the energy of the carbon hexagonal plane, n_{Zr} is the number of Zr atoms on the supercell, and E_{Zr} is the energy of a zirconium atom. The coverage ratio Zr/C is defined as the number of zirconium atoms divided by the number of carbon atoms inside the supercell. These binding energies are also shown below the geometries in Fig. 1 and for some cases the binding energies per Zr atom are given in Table III.

TABLE III. Binding energies per Zr atom on graphene (in eV). For the same coverage, the homogeneous values are always given while the clustered values are within parenthesis separated by dashes according to the metastable states. These geometries of the zirconium atoms are shown in Fig. 1. The highest binding energy is for a mixed configuration of hollow-top atoms at a coverage Zr/C=0.375, with 6.08 eV.

	Position		
Zr/C coverage	Hollow	Bridge	Top
0.056	3.06	2.32	2.24
0.167	4.51 (4.63)	3.96	3.91 (4.71/4.55)[a]
0.500	4.66	5.06	5.20

[a]Clustering in void/centered position.

A. Low coverage: clustering and stability of hollow Zr positions

At low coverage, we study the Zr/C coverage ratios 0.056 and 0.111 with the geometries shown in Fig. 1. At small coverages of the graphene surface, Zr/C=0.056, the most stable configuration for a Zr atom is the hollow position. This position becomes more stable than the bridge by 0.75 eV and than the top by 0.83 eV. Thus, the energy barrier to jump between hollow states can be estimated of at least 0.75 eV. We would like to emphasize that the top configuration was achieved by sinking 0.2 Å the C atom below the Zr in the initial geometry. Without this initial configuration, starting with all the coordinates of the C atoms at the same height, we found that the top configuration is unstable. The energy difference between the top-hollow configurations is large enough to maintain a Zr atom on hollow position at low temperatures. However, there will be diffusion at room temperature, as seen in Sec. VI.

Now, at the coverage Zr/C=0.111, we add an atom close the first one or uniformly distributed. We found that the clustered position, with an atom next to the other, has an energy gain of 0.75 eV with respect to the homogeneous case with atoms in hollow positions. For dimers, we do not reach the top and bridge configuration because these are saddle points in the energy landscape. That is so, even when sinking the surrounding C atoms.

B. Medium coverage: Zr moves to top positions

When we add a third Zr atom to graphene, at a Zr/C coverage ratio of 0.167, the clustered cases remain as the most stable geometries. Surprisingly the most stable cluster lies now on top position with an energy difference of 0.6 eV compared to the homogeneous hollow positions. The hollow and top Zr_3 clusters without a C atom in the center (Fig. 1) are separated by a total-energy difference of only 0.24 eV. The energy difference between the hollow and carbon-centered top trimer is also 0.24 eV. Between both cases the hollow trimer is more stable.

As these energy differences between configurations decrease for the Zr_3 trimer, it seems probable that the top positions can be reached from the previous hollow ones in an atom-by-atom growth process. The trimers would move at room temperature over the graphene plane until they collide

with another Zr or a group of Zr atoms. It is clear that the Zr atom has a trend to cluster over the graphene and it seems that the Zr-trimer cluster could be already a better diffusion unit (see Sec. VI).

We compare the Zr-graphene binding energies with the formation energies of Zr_2, Zr_3, and ZrC molecules. We compute the formation energies of Zr_2, Zr_3, and ZrC molecules as

$$E_F = -(E_{\text{molecule}} - \sum E_{\text{atoms}}). \quad (2)$$

The total formation energies are 8.79 and 4.40 eV for the Zr trimer and the Zr dimer, respectively. The formation energies are large compared with the adsorption energies or the binding energies of the Zr on graphene. This points to the importance of Zr-Zr interaction. The formation-energy difference per zirconium atom between dimer and trimer is 0.73 eV. The Zr trimer is more stable than the Zr-dimer molecule. This difference confirms the previously commented trend to form Zr_3 clusters on graphene.

C. Zr/C coverage ratio=0.375: more favorable coverage

With our cells, coverage ratios between 0.167 and 0.5 could not be considered to have the Zr atoms homogeneously distributed. In fact, the Zr atoms could be arranged in a bunch of different geometries. We center here on the study of the 0.375 coverage ratio which corresponds to 12 Zr atoms per 32 carbon atoms in a graphene 4×4 supercell: four Zr atoms are in hollow positions and eight are on top positions. The Zr-Zr distance is 2.94 Å, which is close to the Zr-Zr distance for the relaxed hexagonal free plane (0001) of zirconium, 2.86 Å. Also the C-C distance in the graphene layer 1.46 Å is not strongly modified from the ideal distances of graphene, 1.43 Å, without zirconium interaction. Thus, the stress and the deformation between planes of the cell are small, leading to the coverage with the highest binding energy per atom, 6.08 eV as seen in Table III. For other geometries or coverages, the binding energies are smaller due to the expansion or contraction of the C/Zr cell. The Zr/C coverage ratios around 0.375 are probably the target for the clustering process. This coverage seems to be the optimal one.

D. High coverage

When we increase the Zr/C coverage ratio up to 0.5, the top position remains as the most stable configuration. The largest binding energy per Zr atom is 5.2 eV. We can compare this binding energy with that of Zr atom in a Zr plane. Such binding energy is defined as

$$E_B = -\frac{E_{\text{Zr-plane}} - n_{\text{Zr}}E_{\text{Zr}}}{n_{\text{Zr}}}, \quad (3)$$

where $E_{\text{Zr-plane}}$ is the energy of a hexagonal (0001) plane of Zr atoms. Using the previous equation, we performed simulations of a frozen coordinate hexagonal plane of zirconium with the same cell and the same positions on the top configurations. The binding energy of a Zr atom as part of a hexagonal Zr plane with fully relaxed coordinates and cell vectors is 5.40 eV. We compare with the binding energy of the Zr hexagonal layer to graphene, 5.08 eV. We found that the Zr-Zr binding energies compete with the one between C and Zr layers. The binding energy of zirconium with their zirconium neighbors in the plane is larger than with the graphene sheet. In fact, the Zr-Zr interaction is much more important at high coverages than the Zr-C interaction. This result agrees with the large strain between Zr and C layers at the 0.5 coverage.

At higher Zr/C coverage ratios, the stress for commensurate structures between planes grew so large that the graphene layer breaks. When the coverage is larger than 0.5, the system relax to form a sort of Zr carbide. This finding suggests that we can set a limit for the maximum Zr/C coverage ratio about 0.5.

E. Atom-by-atom coverage mechanism

When changing coverage, some further scheme serves us to summarize our previous binding-energy study and to comment the growth of Zr layers on graphene. (a) Single Zr atoms and Zr dimers on graphene adsorb in hollow positions. (b) A third atom ends at hollow position next to the first ones and they form a Zr_3 cluster. This trimer moves to top positions, as it seems that their energy barrier is very small at room temperature. In fact, the Zr_3 top-void centered geometry is the most stable as shown in Fig. 1. (c) The Zr-growth process on graphene continues up to a 0.375 Zr/C coverage ratio with the highest Zr-C binding energy. Although our simulations show that a system with a Zr/C coverage ratio of 0.5 is stable, this configuration suffers more stress than our geometrical configuration with a 0.375 Zr/C ratio.

V. ELECTRONIC ORIGIN OF THE LARGE VARIATIONS IN ZR-C DISTANCES AND BINDING ENERGIES WITH COVERAGE

We wish to discuss in more detail the strong change in Zr-C distances and binding energies with coverage. We start out from our basic result of the electronic structure using the projected density of states (PDOS) for the top and hollow configurations in the 0.056 Zr/C coverage ratio, taken as an example. Then, we also study the charge transfer between atomic species and the spin polarization in each atom as a function of coverage by Mulliken population analysis. In the discussion of these electronics properties, we describe the properties of Zr-graphene bond.

A. Role of 5*s* orbitals in Zr and $2p_z$ in graphene

Figure 2 shows the PDOS on the p_z levels of carbon atoms and the *sd* levels of Zr atoms. In the hollow case, the $4d_{x^2-y^2}$ and $4d_{xy}$ orbitals are degenerated and occupied. The $4d_{xz}$ and $4d_{yz}$ orbitals are also degenerated but they are empty as well as the 5*s*. The $4d_{z^2}$ orbital is occupied states and lies close to the Fermi level. In the top configuration all orbitals are present and partially occupied near the Fermi level, including the 5*s*. However, the $4d_{x^2-y^2}$ and $4d_{xy}$ orbitals have the smallest peaks near the Fermi level. The interaction between the zirconium and carbon atoms is partially covalent and comes mainly from the 4*d* orbitals of Zr with the $2p_z$ orbitals of graphene.

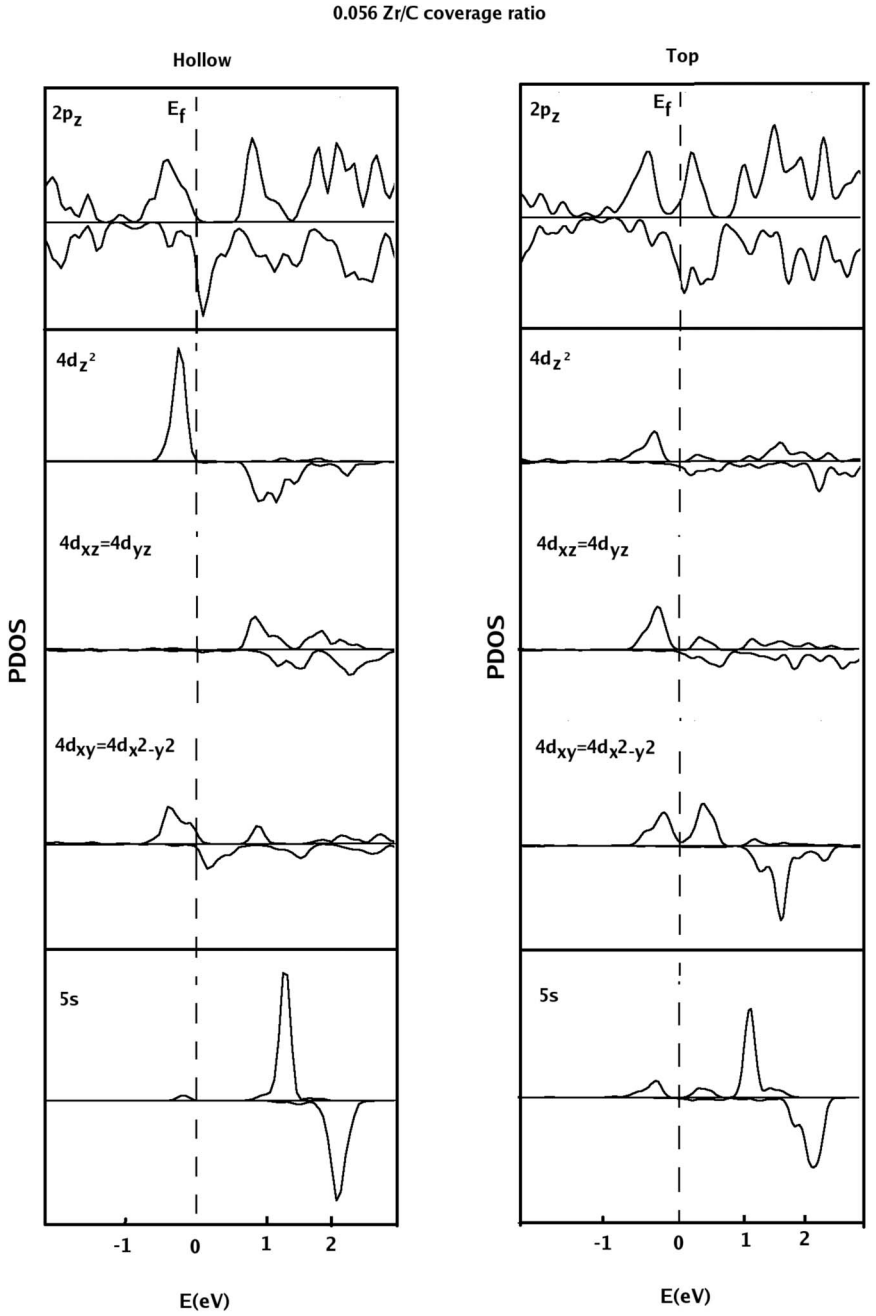

FIG. 2. PDOS at the 0.056 Zr/C coverage ratio in hollow and top positions. Positive and negative values refer to spin up and down, respectively. The vertical dashed line is the Fermi energy. Orbitals and degeneracies are indicated inside the plot. Note that the occupied *s* Zr PDOS is small.

B. Zr-C charge transfer

Our Mulliken population analysis gives valuable data about orbital population and spin polarization. We can allocate charges in the different atomic orbitals. Then, we can study the charge transfer at different Zr/C coverages and configurations and know which orbitals are involved in the bonding process. The charge transfer versus coverage is shown in Fig. 3. The points at 0.056, 0.110, and 0.500 Zr/C coverage ratios are in hollow positions, and the point with 0.375 Zr/C coverage ratio is a hollow/top configuration with a ratio of 1/2, as shown in Fig. 1. The charge transferred per Zr atom decreases at large coverage. In Fig. 3 we see that the extra charge per carbon atom reaches a constant value when the charge transfer per zirconium decreases. This limit show, as expected, a maximum charge that the graphene could accept per C atom. In other words, the graphene plane accepts only certain amount of charge as we increase coverage. We also performed a Mulliken population analysis in all the configurations at each coverage. The charge transfer does not highly depend on the adsorption position. The differences for the charge transfer between hollow, top, and bridge configurations are within 10%. In every case, the integration of the Mulliken populations shows how the charge transfer moves

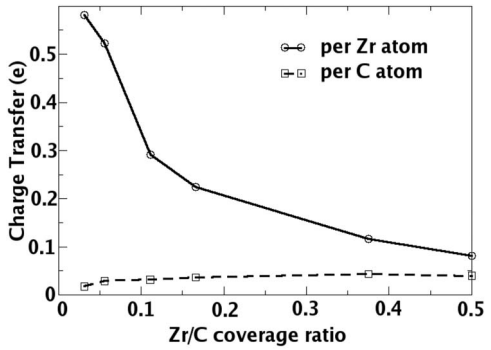

FIG. 3. Charge transfer versus Zr/C coverage ratio. The points at 0.056, 0.110, and 0.500 Zr/C coverage ratios are hollow positions, and the point with 0.375 Zr/C coverage ratio is a mixed hollow/top configuration with a ratio of 1/2 as shown in Fig. 1. When increasing Zr/C ratio, the carbon charge per atom tends to a constant value.

from the 5*s* Zr orbital to the graphene $2p_z$ orbitals. This extra charge in graphene layer becomes delocalized. The charge transfer is clear as with other early transition metals on fullerenes, such as La,[18] because it comes from the charge transfer of *s*-*d* electrons to the C.

C. Spin polarization

As explained in the previous section with the Mulliken population analysis we are also able to study the spin polarization of every orbital in the system. Combining PDOS and Mulliken population analysis, we obtain the information about how the orbitals are locally populated. Non-null spin polarization is found only at 0.056 and 0.5 Zr/C coverage ratio. The spin polarization in all the configurations and coverages comes mainly from the 4*d* orbitals of Zr. The magnetization at 0.056 Zr/C coverage ratio on hollow and top positions is slightly larger than 2 μ_B per zirconium. This Zr magnetic moment is in agreement with the values found for Ti covering nanotubes,[19] graphene and graphene nanoribbons.[20] The carbon atoms in this case contribute around 0.20 μ_B more. With 0.5 Zr/C coverage ratio the magnetization is just about 0.2 μ_B per Zr atom. The spin-density plots at a 0.056 Zr/C coverage ratio in hollow and top geometries are shown in Fig. 4. It is cut at one tenth of the maximum spin-charge difference for the hollow geometry; and at one fifth, for the top geometry. In Fig. 4, we see how the spin density has a $4d_{z^2}$ shape in the hollow case while a mixture

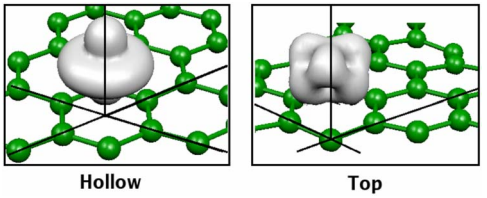

FIG. 4. (Color online) Spin density at 0.056 Zr/C coverage ratio in the hollow and top geometries. The surface is a cut of the maximum spin-charge difference at a tenth for the hollow case and at a fifth for the top. See the d_{z^2} form mainly for the hollow configuration and the mixed *d* form for the top one.

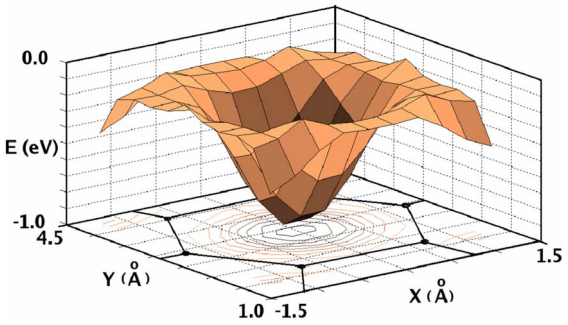

FIG. 5. (Color online) Total energy mapping of Zr atom on graphene surface.

of 4*d* shapes is found in the top geometry. These images are coherent with the PDOS analysis made already in Fig. 2. We are not pursuing any further this objective here. Anyhow spin polarization for transition metals in graphene has been already commented in other work,[23] and it is still an intriguing subject.

VI. DIFFUSION-ENERGY BARRIERS FOR ZR ATOM AND ZR TRIMER

As already said, the energy differences between several positions of Zr atoms given in the previous sections motivate the following study of diffusion energy barriers on graphene. In Secs. III A and III B, the energy differences show that the hollow positions are preferred at low coverages while top positions are more stable at higher coverages. The small energy differences aim us to look at the Zr-trimer cluster diffusion over the graphene layer. While the smallest energy difference between configurations is for the Zr trimer, we also calculated the single Zr atom on graphene to know how stable the hollow position at low Zr/C coverages is. Our calculations have been done in a 3×3 graphene supercell. We change the convergence criteria since we study variations in the total energy within the same supercell. We used a mesh cutoff of 150 Ry and 4 *k* points in the IBZ.

A. Total energy mapping of a Zr atom on graphene surface

In these calculations, we fix the coordinates of two C atoms, away from the absorbed Zr atom, in the graphene surface with the previously calculated and relaxed distances. The two fixed atoms neglect the movement of the graphene center-of-mass during relaxations. We relax all the other C atoms. We nullify the forces of the Zr atom in the *x* and *y* axes at every step while the *z* coordinate is relaxed. The total-energy mapping of the Zr atom on a graphene surface is shown in Fig. 5.

The Zr top positions become unstable in this energy-mapping calculation. In the previous sections, the top position was achieved as a metastable state because we have purposely sunk the C atom under the Zr in the input geometry. When starting with all the C atoms at the same height, as in Fig. 5, the top configuration is unstable. The bridge position in Fig. 5 is also a saddle metastable point. Otherwise the energy differences between hollow, bridge, and top posi-

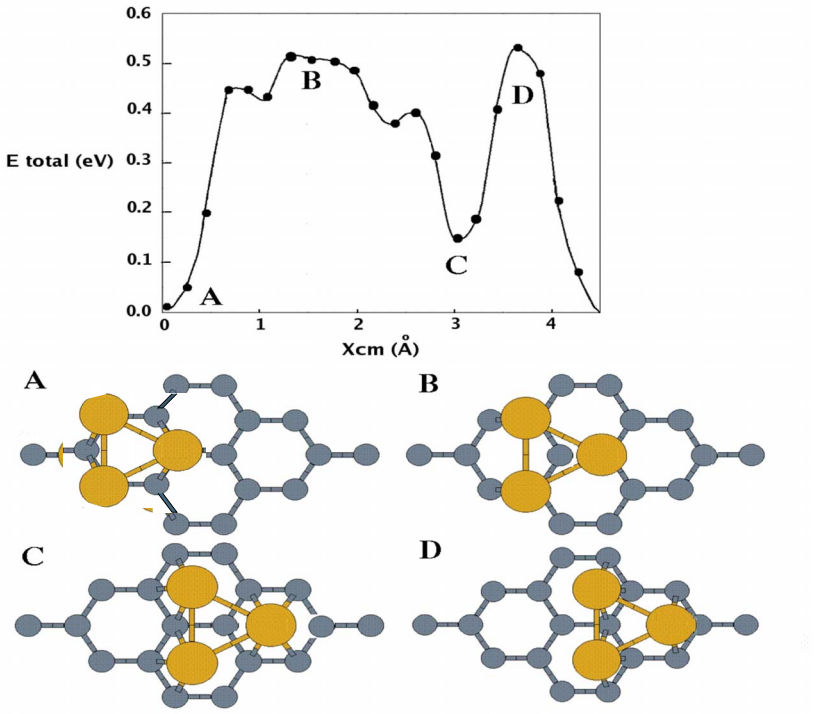

FIG. 6. (Color online) Total energy versus $x_{\text{center-of-mass}}$ position of the Zr_3 cluster on graphene layer. Geometry snapshots are also given.

tions found in Fig. 5 are consistent with previous results. The minimum-energy barrier between two hollow positions is close to the bridge configuration. The diffusion energy-barrier height for Zr atom on graphene is about 0.75 eV, which is in full agreement with the value found for Ti in graphene nanoribbons.[20] Although similar, the larger value compared with the diffusion of C adatoms on graphene, about 0.5 eV,[17] indicates the different type of bond, as already explained in the previous section.

B. Diffusion-barrier calculations for Zr trimer on graphene

Next, we show the results for Zr-trimer diffusion on graphene. The calculation of diffusion energy barriers has been performed with the same convergence criteria used above for the Zr atom. We fix two carbon atoms of the graphene, away for the trimer, to neglect the movement of graphene as a whole. We relax the other C atoms in all directions. Now we define a relative distance between the Zr trimer and the graphene center of masses. The Zr_3 center-of-mass position is constrained to move between two top-void centered positions while the coordinates of the Zr atoms are relaxed. We map the diffusion along this high-symmetry direction. The total energies versus the different Zr-trimer center-of-mass positions are given in Fig. 6.

Figure 6 shows the highest energy barrier for points B and D in a hollow and a top configuration with the carbon atom inside, respectively. An intermediate valley is close to have Zr atoms in the hollow configuration, point C in Fig. 6. The energy differences between the A-B configurations have close values to those in Fig. 1. The energy barrier about 0.5 eV between hollow states peaks around the void centered top position. With this barrier value, diffusion occurs for the Zr_3 clusters at room temperature. The diffusion-energy barrier for Zr_3 clusters is smaller than for the single atom.

C. Some considerations on Zr adatoms in graphene vacancy defects

As we remarked above in the introduction, when metal atoms of clusters move experimentally between substitutional positions in graphene, the activation energy can be estimated.[13] For atoms or clusters of Au and Pt, the activation energies and location are connected by the relation $D=\langle r^2\rangle/(4t)$, where t is the time, D is the diffusion coefficient, and r corresponds to the hopping distance by the atom or cluster. Using experimental HRTEM images and the previous equation, the activation energy is $E_a \sim 2.5$ eV for both atoms and clusters of Au or Pt on graphene. For nanotubes, Gan *et al.*[13] have shown that the activation energy is ~ 2.3 eV. The activation energy for nanotubes is slightly smaller than that for graphene. The large value of the activation energy in both cases point to strong metal-carbon covalent bonds. We shall discuss briefly below for the case of a lattice vacancy, the change in the Zr absorption and diffusion energies due to the presence of a vacancy defect. Note that in the early transition metals, such as Zr, we have to take also into account the d electrons participating in the bond as in Au and Pt.

We have considered a vacancy in the 3×3 graphene cell shown in Fig. 1. We have deposited Zr atoms on the graphene cell and relaxed the geometry until the forces converged to the previous limit. The relaxed geometries are shown in Fig. 7.

By looking at the initial geometries several issues can be commented. When we start with Zr atoms on hexagons, the Zr atom relaxes to the closest hollow position. Its description is completely similar to the previous hollow case in graphene at low coverages Zr/C=0.056. In this case, the vacancy in-

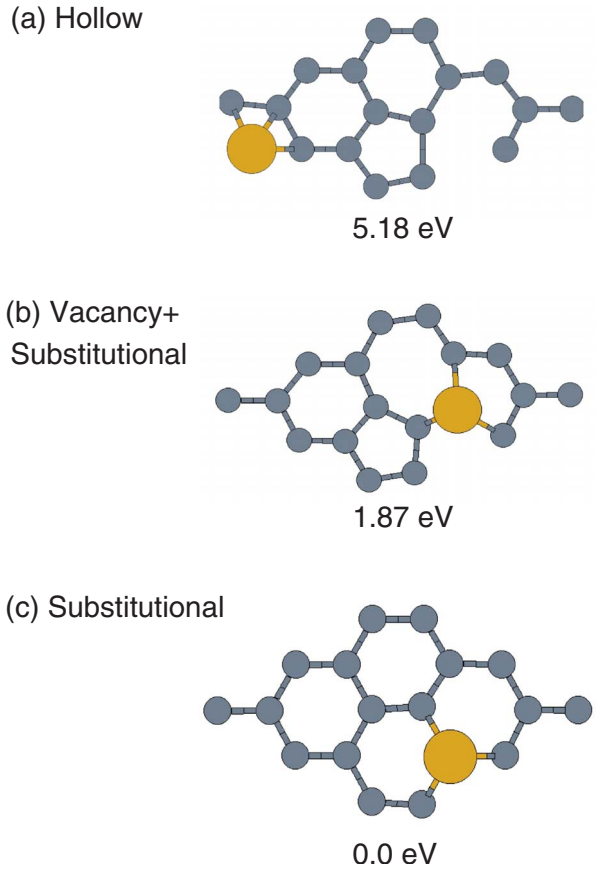

FIG. 7. (Color online) Dopping of graphene with Zr in the presence of vacancies. The energies relative to the ground state are given under the geometries. To remark the difference in the stronger pentagon new bond for the middle geometry when the Zr atom is on the vacancy.

deed reconstructs, as usual it ends in a pentagon, with a long C-C bond distance, 1.67 Å, and a void with goggles form. For Zr atom on top of the unreconstructed vacancy, the metal atom remains there, and the vacancy did not reconstruct. The simplest way to check the effect of metals on the vacancy reconstruction was to start from Zr close to the relaxed vacancy. We have seen that on the pentagon of the reconstructed vacancy, the Zr atom moves largely to a substitutional position in one goggle. It moves even from the hollow position, open a C-C bond, and the C-C distance of the pentagon becomes smaller, 1.47 Å, i.e., stronger.

The results of the energy differences respect to the ground state are also given in Fig. 7. The lower energy is for the Zr forced to be in substitutional position. The next low-lying position with Zr on the goggles is around 2 eV. In both substitutional positions, the Zr atom is bound more covalently to the close C atoms. The nearest-neighbor distances are around 2.05 Å, smaller that previous ones calculated for Zr on graphene. The charge transfer is almost the same about 0.69 and 0.58 electrons for positions (b) and (c), respectively.

The energy difference between both (b) and (c) positions is anyhow lower than C-C binding energy. The lower energy (c) substitutional position is only reached when breaking the stronger 1.47 Å C-C pentagon bond in (c) geometry. We can think that the vacancy stronger bond in (b) erects a potential barrier for the Zr atom and therefore implies kinetically a stable position. Then it could be assumed that the activation energy for Zr atom moving on graphene can be estimated by summing the energy difference between (a) and (b) panels in Fig. 7, 3.31 eV, to the previous barrier energy between hollow positions, 0.75 eV. The obtained value of about 4 eV is clearly larger than previous experimental activation energies for Au and Pt about 2–3 eV. We concluded that early transition metals have a lower diffusivity due to the stronger bonds with C. For the temperatures of the experiment, 600 °C, the Zr atoms would remain anchored to the carbon defects. As commented in the previous section, only diffusion of adatoms and clusters without close defects will happen but we need smaller temperatures and longer times so that the diffusion could be seen by HRTEM. This pinning of Zr atoms in vacancies is similar to the high stability of substitutional Ni atoms in graphenic systems reported in previous experimental and theoretical works.[21–23] It remains to be seen if clustering of dimers and trimers, already known from previous subsections to weak the Zr-C bonds, would be able to low also the activation barriers in defects and to favor diffusion. However, these calculations require larger cells and they are beyond the scope of this work.

VII. DISCUSSION AND SUMMARY

We have simulated several geometrical configurations and coverages of zirconium adsorbed on a graphene layer. The energy barriers for Zr atom and for Zr_3 cluster on graphene were also calculated.

We see that the Zr adsorption on graphene induces a variation on the C-C bond lengths. The changes are driven by Zr strain. At high coverages, the C-C distances expand or compress to accommodate the Zr-Zr atoms at equilibrium. The absorbed Zr atoms change the height of the nearest C atoms. In every case we found that the graphene deformation occurs sinking the C atoms under the Zr atoms. The maximum sink corresponds to top adsorption and it is as large as 0.32 Å for the C atom under the Zr.

We calculated the binding energies for every geometry. The largest binding energy of zirconium on graphene corresponds to a Zr/C coverage ratio of 0.375. The optimum Zr configuration is commensurate with graphene. This configuration has 12 Zr atoms with a ratio of 2/1 for top/hollow positions. The binding energy for this configuration becomes large because there is no stress between both planes. This binding energy is larger than that per zirconium atom on the free-standing relaxed hexagonal plane.

We found that the clustering of Zr atoms on graphene is energetically more stable than the homogeneous distribution. We explained these facts because the Zr-Zr bond is stronger than the Zr-C bond. At the Zr/C coverage ratio of 0.166, the energy differences between the different atomic configurations of the Zr_3 cluster are small, around 0.48 eV between maximum and minima. This finding indicates that diffusion between hollow and top positions for the Zr_3 cluster at room temperature could happen. Although further research is needed for understanding the Zr diffusion over the graphene, the Zr_3 cluster could be likely the "diffusion unit." We ex-

plain this with the energy barriers for Zr atom and Zr_3 cluster discussed in Sec. V. The diffusion-energy barriers for trimers are small. This diffusion probably leads to clustering on graphene. The fact that the Zr cohesion with graphene vacancies, on the other hand, is at least 4 eV, has shown the strong Zr-C bond. With this cohesion energy, it would be difficult to move the substitutional Zr atoms at the experimental HR-TEM temperatures[13] in order to see atoms diffusing on graphene.

At Zr/C 0.5 coverage ratio the top position becomes the most stable but its binding energy is smaller than for the previous Zr/C coverage ratio of 0.375. This gives a coverage limit between the 0.375 and 0.5 Zr/C coverage ratios. A crossover between hollow and top states, more stable at lower and higher coverages, respectively, could be around the coverage ratio $Zr/C=0.375$.

From the Mulliken population analysis, we found that the charge transfer to graphene comes from the 5*s* orbitals of the zirconium in all cases. The accepted charge per carbon atom is nearly steady with the coverage. The spin polarization comes from the 4*d* orbitals and happens at small coverages in the hollow or the top positions. The local spin polarization of the Zr site is around 2 μ_B. These electronic findings explain the large variations in C-Zr distances and binding energies.

All these simulations give valuable results about the behavior of the adsorption of Zr on graphene. To sum up, the main result is that the Zr/C coverage ratio of 0.375 is preferred. The calculations about the diffusion energy barriers for the single Zr atom and the Zr_3 trimer show that these barriers are not large, especially for the trimer. Also a trend to cluster the Zr atoms on graphene is found and always the cluster configuration is energetically more stable than the homogeneous one. The high number of configurations simulated shows that the nature of the Zr-C bond remains ionic while losing the covalent character, when changing the coverage ratio Zr/C from 0.056 to 0.5.

ACKNOWLEDGMENTS

This work was supported by the Basque Government through the NANOMATERIALS under Project No. IE05-151 under the ETORTEK Program (iNanogune), Spanish Ministerio de Ciencia y Tecnología (MCyT) of Spain (Grant No. Fis2007-66711-CO2-02 and MONACEM project) and University of the Basque Country (Grant No. IT-366-07). The computing resources from the Donostia International Physics Center (DIPC) and the SGI-SGIkerUPV are gratefully acknowledged. We thank the INASMET team (N. Garmendia, R. Muñoz, and I. Obieta) for discussions.

[1] S. Ijima, Nature (London) **354**, 56 (1991).
[2] J. S. Arellano, L. M. Molina, A. Rubio, and J. A. Alonso, J. Chem. Phys. **112**, 8114 (2000).
[3] R. H. Baughman, A. A. Zakhidov, and W. A. de Heer, Science **297**, 787 (2002).
[4] J. Robertson, Mater. Today **7**, 46 (2004).
[5] G. L. Hwang and K. C. Hwang, J. Mater. Chem. **11**, 1722 (2001).
[6] E. Flahaut, A. Peigney, Ch. Laurent, Ch. Marliere, F. Chastel, and A. Rousset, Acta Mater. **48**, 3803 (2000).
[7] J. Sun and L. Gao, J. Electroceram. **17**, 91 (2006).
[8] N. Garmendia, L. Bilbao, R. Muñoz, L. Goikoetxea, A. García, I. Bustero, B. Olalde, N. Garagorri, and I. Obieta, Key Eng. Mater. **361**, 775 (2008).
[9] F. Lupo, R. Kamalakaran, C. Scheu, N. Grobert, and M. Rühle, Carbon **42**, 1995 (2004).
[10] Lei Huang, S. P. Lau, Y. B. Zhang, B. K. Tay, and Y. Q. Fu, Nanotechnology **15**, 663 (2004).
[11] Y. Shan and L. Gao, Nanotechnology **16**, 625 (2005).
[12] Y. Sanchez-Paisal, D. Sanchez-Portal, N. Garmendia, R. Muñoz, I. Obieta, J. Arbiol, L. Calvo-Barrio, and A. Ayuela, Appl. Phys. Lett. **93**, 053101 (2008).
[13] Y. Gan, L. Sun, and F. Banhart, Small **4**, 587 (2008).
[14] J. M. Soler, E. Artacho, J. D. Gale, A. Garcia, J. Junquera, P. Ordejon, and D. Sánchez-Portal, J. Phys.: Condens. Matter **14**, 2745 (2002).
[15] J. P. Perdew, K. Burke, and M. Ernzerhof, Phys. Rev. Lett. **77**, 3865 (1996).
[16] A. Ayuela, G. Seifert, and R. Schmidt, Z. Phys. D: At., Mol. Clusters **41**, 69 (1997).
[17] P. O. Lehtinen, A. S. Foster, A. Ayuela, A. V. Krasheninnikov, K. Nordlund, and R. M. Nieminen, Phys. Rev. Lett. **91**, 017202 (2003).
[18] G. Seifert, A. Bartl, L. Dunsch, A. Ayuela, and A. Rockenbauer, Appl. Phys. A: Mater. Sci. Process. **66**, 265 (1998).
[19] E. Durgun, S. Dag, V. M. K. Bagci, O. Gülseren, T. Yildirim, and S. Ciraci, Phys. Rev. B **67**, 201401(R) (2003).
[20] H. Sevinçli, M. Topsakal, E. Durgun, and S. Ciraci, Phys. Rev. B **77**, 195434 (2008).
[21] M. Ushiro, K. Uno, T. Fujikawa, Y. Sato, K. Tohji, F. Watari, W. J. Chun, Y. Koike, and K. Asakura, Phys. Rev. B **73**, 144103 (2006).
[22] F. Banhart, J. C. Charlier, and P. M. Ajayan, Phys. Rev. Lett. **84**, 686 (2000).
[23] E. J. G. Santos, A. Ayuela, S. B. Fagan, J. Mendes Filho, D. L. Azevedo, A. G. Souza Filho, and D. Sánchez-Portal, Phys. Rev. B **78**, 195420 (2008).